

Jahn-Teller Spectral Fingerprint in Molecular Photoemission: C₆₀

Nicola Manini* and Paolo Gattari

Dipartimento di Fisica, Università di Milano, Via Celoria 16, 20133 Milano, Italy and INFN, Unità di Milano, Milano, Italy

Erio Tosatti

*International School for Advanced Studies (SISSA), Via Beirut 4, 34014 Trieste, Italy
INFN Democritos National Simulation Center, and INFN, Unità Trieste, Italy and
International Centre for Theoretical Physics (ICTP), P.O. Box 586, 34014 Trieste, Italy*

(Dated: November 14, 2018)

The h_u hole spectral intensity for $C_{60} \rightarrow C_{60}^+$ molecular photoemission is calculated at finite temperature by a parameter-free Lanczos diagonalization of the electron-vibration Hamiltonian, including the full 8 H_g , 6 G_g , and 2 A_g mode couplings. The computed spectrum at 800 K is in striking agreement with gas-phase data. The energy separation of the first main shoulder from the main photoemission peak, 230 meV in C_{60} , is shown to measure directly and rather generally the strength of the final-state Jahn-Teller coupling.

PACS numbers: 33.60.-q, 33.20.Wr, 71.20.Tx, 36.40.Cg

Photoemission (PE) from a closed-shell high-symmetry molecule, involving Jahn-Teller (JT) effect in the final state, is accompanied by characteristic vibronic structures in the measured hole spectrum [1]. Although accurate spectral calculations have recently appeared in the chemical literature, e.g. for benzene [2], there still is a strong need for a qualitative understanding of a more general nature, possibly system independent, and informative on the nature and the strength of the JT coupled problem. A recent case in point is that of gas-phase C_{60} , where an important side peak was reported 230 meV above the main PE peak [3, 4] (see Fig. 1). As this excitation energy is in fact larger than all vibrational frequencies of C_{60} (32-197 meV), its nature could not be straightforwardly interpreted, leading to a debate [5].

In this Letter we present first of all a detailed understanding of the PE structures that are accurately reproduced for $C_{60} \rightarrow C_{60}^+$ (Fig. 1) through calculations that fully include temperature and that contain no adjustable parameters. By taking further this calculation to pieces, we identify the important ingredients that determine the spectrum. The first is symmetry selection: the initial orbital symmetry dictated by the suddenly injected bare hole extends to the whole spectrum. The second is a property of weakly coupled JT vibronic multiplets that requires the first excitation energy of the same symmetry as the ground state (GS) to rise above the bare vibration energy by an amount strictly proportional to the squared JT coupling. Specifically in C_{60}^+ , symmetry requires the 230 meV peak to correspond to an h_u vibronic excitation above the h_u GS. JT transforms the highest $H_g^{(8)}$ vibration ($\hbar\omega < 200$ meV) of C_{60} into an h_u vibron near 230 meV. Interestingly, the 20% magnitude of this upward shift fingerprints quite accurately the medium-sized overall JT coupling of C_{60} . As both properties above are apparently general, and since the upward shift tracks the

coupling intensity well beyond the weak-coupling limit, this kind of analysis appears of much more general value. In particular, the first vibronic excitation energy as seen in PE of other weak to medium JT-coupled molecules should and does gauge their respective couplings as well.

We adopt for C_{60} the simplest model [7, 8, 9] describing the JT coupling of the orbitally degenerate h_u

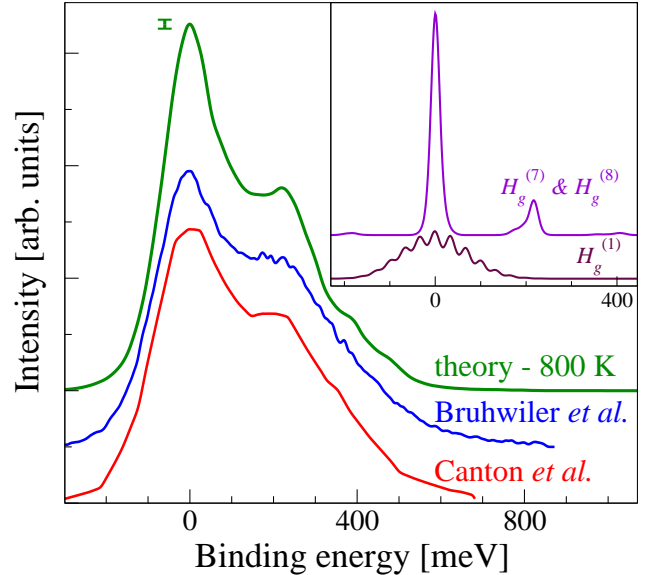


FIG. 1: Experimental PE spectra by Canton *et al.* [4] and by Brühwiler *et al.* [3] compared with the calculation based on the *ab initio* parameters of Ref. [6] ($T = 800$ K, $N_{\text{tier}} = 31$, $N_{\text{max}} = 10^5$, $N_{\text{sample}} = 245$). Intensities are normalized to unity. Inset: $T = 800$ K spectra including the single $H_g^{(1)}$ mode, and $H_g^{(7)}$ and $H_g^{(8)}$. All spectra are shifted to move the main peak to zero energy and broadened with a 10 meV HWHM Gaussian. The errorbar gives the largest statistical error introduced by random sampling of the initial states.

hole with the molecular vibrations. The linear JT coupling is nonzero for two nondegenerate A_g , six fourfold-degenerate G_g and eight fivefold-degenerate H_g vibration modes, or 66 vibrations altogether [7, 8, 10]. The resulting $h \otimes (A + G + H)$ JT Hamiltonian thus consists of the fivefold h_u highest occupied molecular orbital (HOMO), of 66 harmonic oscillators, and of the electron-vibration (e-v) coupling term [6, 8]:

$$\hat{H} = \hat{H}_0 + \hat{H}_{\text{vib}} + \hat{H}_{\text{e-v}}, \quad (1)$$

$$\hat{H}_0 = \epsilon_{\text{HOMO}} \sum_{m\sigma} \hat{c}_{m\sigma}^\dagger \hat{c}_{m\sigma}, \quad (2)$$

$$\hat{H}_{\text{vib}} = \frac{1}{2} \sum_{\Lambda j \mu} \hbar \omega_{\Lambda j} \left(\hat{P}_{\Lambda j \mu}^2 + \hat{Q}_{\Lambda j \mu}^2 \right), \quad (3)$$

$$\hat{H}_{\text{e-v}} = \sum_{\substack{r \Lambda j \mu \\ \sigma m m'}} k^\Lambda g_{\Lambda j}^{(r)} \hbar \omega_{\Lambda j} C_m^{r \Lambda \mu} \hat{Q}_{i \Lambda \mu} \hat{c}_{m\sigma}^\dagger \hat{c}_{m'\sigma}. \quad (4)$$

Here m, μ label components within the degenerate multiplets [8, 11], j counts modes of symmetry Λ , $C_{mm'}^{r \Lambda \mu}$ are Clebsch-Gordan coefficients [11] of the icosahedral group I_h that couple the h_u fermion operators $\hat{c}_{m\sigma}^\dagger$ to a Λ vibration. $\hat{Q}_{i \Lambda \mu}$ are the dimensionless normal-mode vibration coordinates in units of $x_0(\omega_{\Lambda j}) = \sqrt{\hbar/(\omega_{\Lambda j} m_C)}$ where m_C is the mass of the C atom), and $\hat{P}_{i \Lambda \mu}$ the corresponding conjugate momenta. The additional multiplicity $r = 1, 2$, needed for H_g vibrations only, labels the two separate kinds of H_g coupling allowed under the *same* symmetry [6, 11].

In the present calculation we adopt the fully *ab initio* numerical values of the e-v coupling parameters $g_{\Lambda j}^{(r)}$ obtained by a Density Functional (DF) calculation in Ref. [6] [22]. We also use the calculated vibrational frequencies of Ref. [6], that are close to the experimental frequencies of the A_g and H_g modes, but also cover the experimentally unavailable or unreliable G_g modes. E-v couplings are dimensionless, each of them normalized to its respective vibration quantum, so as to reflect directly the relative coupling strength. Numerical factors $k^{A_g} = \frac{5\frac{1}{2}}{2}$, $k^{G_g} = \frac{5\frac{1}{2}}{4}$, $k^{H_g} = \frac{1}{2}$, are included to make contact with Ref. [6].

In the sudden approximation, the angle-integrated PE spectrum $I(E)$ is given by Fermi's golden rule [2]

$$I(E) = \frac{1}{10} \sum_{m\sigma i} I_{im\sigma}(\omega) P(i), \quad (5)$$

$$I_{im\sigma}(E) = \sum_f |\langle f | \hat{c}_{m\sigma}^\dagger | i \rangle|^2 \delta(E - E_f + E_i), \quad (6)$$

where $|i\rangle$ represents the starting vibrational eigenstate of neutral C_{60} , of energy E_i , and $|f\rangle$ represents a vibronic JT eigenstate of C_{60}^+ , of energy E_f . $\hat{c}_{m\sigma}^\dagger |i\rangle$ is the initial bare hole, where the spin- σ electron has been ejected from one orbital m of the fivefold degenerate h_u HOMO, but the molecule is still unrelaxed. The factor 1/10 and

the sum over m and σ signifies averaging over the 5 orbital and 2 spin states of the hole. Assuming thermal equilibrium we generate the boson numbers $\{v_{\Lambda j \mu}\}$ of the initial neutral molecule by randomly sampling the probability distribution $P(i) = Z^{-1} \exp(-E_i/k_B T)$, where $Z = \sum_i \exp(-E_i/k_B T)$ and $E_i = \sum \hbar \omega_{\Lambda j} v_{\Lambda j \mu}$. In the present medium-coupling regime we compute the final-state vibronic energies and matrix elements in (6) by numerical Lanczos diagonalization of the Hamiltonian (1) on the product basis of the five h_u states times the harmonic oscillator ladders. Since these contain an infinite number of states, some truncation is necessary. As we generally want to address high temperatures of the molecular beam ($T = 800$ K used for C_{60} , $k_B T \gtrsim 2\hbar\omega$ of the strongly coupled $H_g^{(1)}$ mode) a standard truncation would involve a far too large Hilbert space size. We generate a smarter basis starting from the initial excitation $\hat{c}_{m\sigma}^\dagger |i\rangle$, and iteratively adding sets of states ("tiers") directly coupled to those of the previous tier by matrix elements of $\hat{H}_{\text{e-v}}$, in a scheme inspired by Ref. [12]. This procedure is iterated N_{tier} times so that states relevant at up to $(2N_{\text{tier}})$ -th order in perturbation theory are included [23]. The application of about 350 Lanczos steps [13] generates a tridiagonal matrix, which provides a well converged spectrum.

The basis for the calculation of Fig. 1 includes about 720000 states, in particular all the states generated by up to three applications of $\hat{H}_{\text{e-v}}$ to $\hat{c}_{m\sigma}^\dagger |i\rangle$: the convergence of the truncated basis is quite good. We repeat the whole procedure of basis generation / spectrum calculation for each of the N_{sample} initial states, and average the obtained spectra. The above procedure is carried out including all H_g and G_g modes. The A_g modes separate out, as they can be solved analytically as a simple displaced oscillators, and are included exactly by convolution.

Figure 1 compares the theoretical PE spectrum calculated at $T = 800$ K with the measured spectra by two separate groups. All experimental features, including the characteristically broad and asymmetric main PE peak, the strongest satellite peak around 230 meV, a second weaker peak near 400 meV, and a slow decay up to 600 meV are remarkably reproduced, based purely on *ab initio* parameters. The model and its ingredients thus appear to describe quite accurately the PE spectrum of C_{60} . We can now take it apart, so as to understand the underlying physics to satisfaction.

We address the two main features of the spectrum, namely a) the large broadening and b) the 230 meV peak. By eliminating G_g and A_g modes from the calculation there is no large change in the spectrum. Thus only the H_g modes are important. Among H_g modes, the largest couplings belong to the low-frequency $H_g^{(1)}$ 32 meV quadrupolar radial mode, and to the two high-frequency C-C stretch modes $H_g^{(7)}$ and $H_g^{(8)}$ at $\hbar\omega = 181$

and 197 meV). When we include $H_g^{(1)}$ alone we find (inset) that the thermally broadened asymmetric main peak is well reproduced. Therefore $H_g^{(1)}$ is the main responsible for the large broadening.

When only $H_g^{(1)}$ is included, all satellite structures above 200 meV are absent, and do not reappear even if we arbitrarily increase the $H_g^{(1)}$ coupling to larger and larger values. This rules out the possibility to attribute the 230 meV structure to an “electronic” splitting [5]. As it turns out, electronic JT splittings become visible in experimental PE spectra, such as those of $\text{Fe}(\text{CO})_5$ [14], and in theoretical spectra, like those of Martinelli *et al.* [15] only for very strong e-v coupling, whereas in C_{60} coupling is intermediate at most. That suggests that the 230 meV peak in C_{60} should rather be associated to the high-frequency modes $H_g^{(7)}$ and $H_g^{(8)}$. However, the connection between their frequencies < 200 meV and the 230 meV peak position is far from obvious. To clarify this, we calculate the spectrum by including $H_g^{(7)}$ and $H_g^{(8)}$ alone (inset of Fig. 1). The result is a much narrower spectrum ($H_g^{(1)}$ is now omitted), showing a high-energy satellite at a significantly (10%) higher energy than $\hbar\omega_{H_g}$. This increase in vibronic excitation energy above the purely vibrational $\hbar\omega$ for the $v=1$ -phonon excitation of a trivial displaced oscillator is in fact a characteristic signature of the dynamic JT effect, and can be understood on the basis of symmetry. For $H_g^{(7)}$ and $H_g^{(8)}$, $\hbar\omega$ is almost three times the thermal energy: the main initial-state contribution to the spectrum comes from $|i\rangle =$ the neutral molecule GS, of symmetry A_g . The bare hole $\hat{c}_{m\sigma}^\dagger|i\rangle$ therefore carries the orbital h_u symmetry of the HOMO. This state has nonzero overlap strictly only with final states $|f\rangle$ of the same symmetry h_u . This *single symmetry channel* thus represents the only contributor to the low-temperature PE spectrum according to (6) [24]. The blue shift of the vibronic peak relative to the bare vibration is now due to two general properties (in fact common to all dynamical JT systems): (i) the coupling independence of the *average* excitation energy in any vibronic multiplet at weak coupling (the leading change is of order g^4) [16]; (ii) the increasing “repulsion” that the GS level exerts for increasing g on all excited states of the same symmetry, which pushes them upward.

Both concepts are illustrated in Fig. 2, depicting the vibronic excitation energies (with special attention to the h_u states) for the simplest case of a single H_g mode, as a function of the e-v coupling strength g^2 . The approximate coupling independence of the *average* excitation energy of the multiplet of states derived from the $v=1$ -phonon manifold is apparent. Within this multiplet (made of $h_u \times H_g = a_u + t_{1u} + t_{2u} + 2g_u + 2h_u$), the h_u vibronic states are the sole that have another state of the same symmetry (the GS itself) lower in energy “pushing” them upward. As a result, for small but increasing coupling, the h_u excited vibronic states, move necessarily

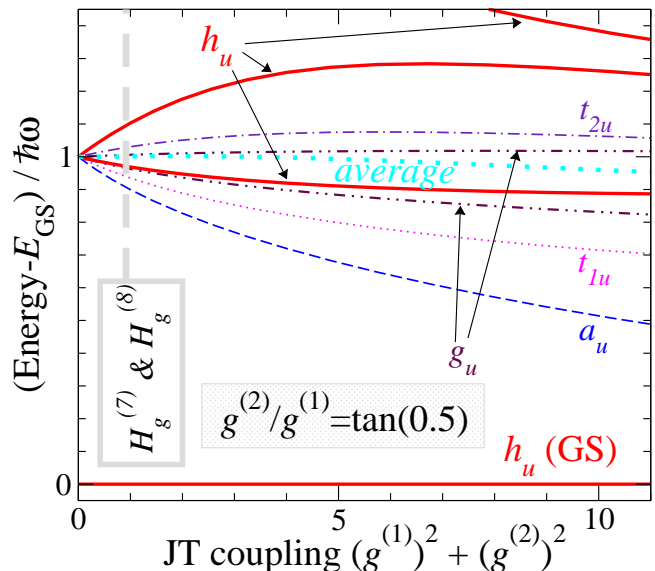


FIG. 2: Vibronic excitation energies for a single H_g mode coupled to the h_u level, as a function of coupling, for a ratio $g^{(2)}/g^{(1)}$ characteristic of the $H_g^{(7/8)}$ modes. The *average* refers to the multiplet originating from the 1-phonon states. Bold: h_u states, the only visible states in $T = 0$ PE.

upward in energy above $\hbar\omega_{H_g}$. Moreover the amount of shift is at weak coupling proportional to g^2 and reflects the strength of the coupling. None of these results seems specific to the $h \otimes H$ JT model of C_{60} . For example, identical conclusions apply to the $e \otimes E$ problem [16]. Indeed a 15% blue shift of the first vibronic satellite is clearly observable in the PE spectra of benzene [17].

In C_{60} we must consider the two high-frequency modes $H_g^{(7)}$ and $H_g^{(8)}$ at $\hbar\omega = 181$ and 197 meV). The couplings for these two modes alone accounts for a 10%, or roughly 20 meV shift of the main $H_g^{(7,8)}$ vibronic satellite above $\hbar\omega$. This is about half of the total observed and calculated shift of ~ 40 meV of the 230 meV satellite relative to $\hbar\omega$. The remainder is a collective effect of all other modes simultaneously interacting with the HOMO, and pushing their respective $v = 1$ satellites (weak and thus invisible at large temperature) upward. All goes as if effectively the coupling of the $H_g^{(7/8)}$ modes were larger, i.e. effectively moving to the right of the vertical dashed line in Fig. 2.

We have thus attained the following understanding of the 800 K PE spectrum of C_{60} : (i) the strong 230 meV satellite (and the weak 400 meV too) is due to h_u -symmetry vibrons derived from $H_g^{(7/8)}$ modes, blue shifted by repulsive coupling to the h_u GS; (ii) the large spectral broadening is due mainly to $H_g^{(1)}$. Clearly, this broadening of the 800 K spectrum prevents direct extraction of further detailed information about the actual e-v couplings of the fullerene cation. Our calculations, when repeated for lower temperatures, indicate a wealth

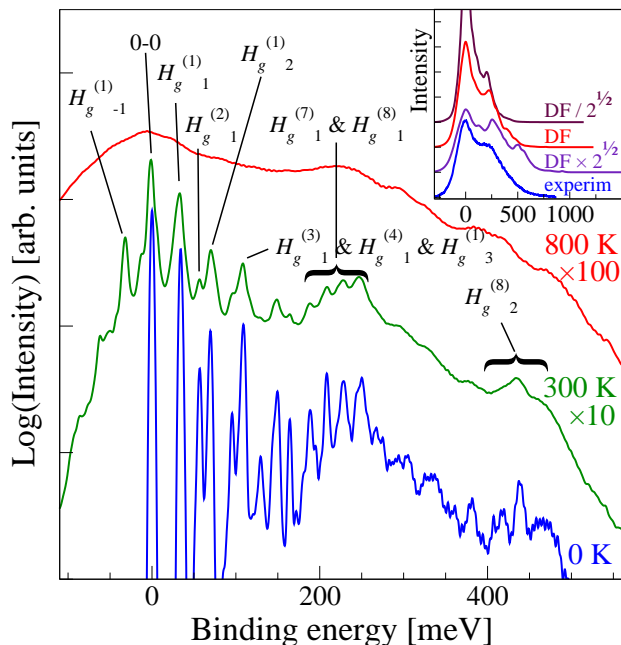


FIG. 3: Temperature dependence of the PE, computed including all modes of C_{60} for $T = 0$, $T = 300$ K and $T = 800$ K. Labels $\Lambda^{(j)}_v$ indicate the leading component in the vibronic states. Inset: computed spectra ($T = 800$ K) based on the same DF coupling parameters $g_{\Lambda_j}^r$ divided by $\sqrt{2}$, original, and multiplied by $\sqrt{2}$, compared to experiment [3].

of structures that should emerge. Figure 3 shows that already a measurement carried out at 300 K would provide enough detail to get precise indications about the couplings of individual modes. For example, the intensity ratios between the main peak and the subsequent peaks at 35 and 65 meV is a direct measure of g_{H_g1} . A cool molecular beam experiment [18] would be extremely useful. Also in view of future cool-beam data it is meaningful to address the question of how accurate the calculated DF e-v couplings used here really are. For t_{1u} electrons coupled to H_g vibrations, the calculated DF couplings were argued for example to be too weak by a substantial amount, by comparison to the larger couplings needed in order to fit C_{60}^- PE [19]. In our HOMO case, the excellent agreement of calculations with experiment suggests that there is no such failure. Figure 3 (inset) shows several PE calculations with rigidly rescaled e-v parameters. Comparison with experiment indicates that the DF couplings are, on the whole, quite close (if slightly on the weak side) to the actual couplings of C_{60}^+ . Much larger JT coupling values like those obtained using different approaches [20] are ruled out. That is very good news, for it gives further confidence in the future possibility to rely solidly on DF for a good description of the intra-fullerene chemical bond, and of its perturbations.

In conclusion, we present here a detailed calculation of the PE spectrum of a high-symmetry molecule, C_{60} ,

which is JT active in its one-hole state. We find excellent agreement with experiment, confirming for the first time the accuracy of the e-v couplings as extracted from DF calculations. Perhaps more importantly, we reach a fresh understanding of the PE spectrum, with its width, its vibronic peak, and the reason for its blue shift relative to the bare vibrations. The blue shift of the one-vibron satellite is argued to represent a more general characteristic fingerprint of JT systems in the weak-to-intermediate coupling regime, and is found for example in the $e \otimes E$ JT of benzene as well.

We are indebted to G.P. Brivio, P. Brühwiler, A. Del Monte, D. Galli, M. Lueders, L. Molinari, G. Onida, F. Parmigiani, A. Parola, and G.E. Santoro, for useful discussion. This work was supported by the European Union, contracts ERBFMRXCT970155 (TMR FULPROP) as well as by MIUR COFIN01, and FIRB RBAU017S8R operated by INFN.

* Electronic address: nicola.manini@mi.infn.it

- [1] R. Lindner *et al.*, *Science* **271**, 1698 (1996).
- [2] H. Köppel *et al.*, *J. Chem. Phys.* **117**, 2657 (2002).
- [3] P. Brühwiler *et al.*, *Chem. Phys. Lett.* **279**, 85 (1997).
- [4] S. E. Canton *et al.*, *Phys. Rev. Lett.* **89**, 045502 (2002).
- [5] N. Manini and E. Tosatti, *Phys. Rev. Lett.* **90**, 249601 (2003); S. E. Canton *et al.*, *ibid.*, 249602.
- [6] N. Manini *et al.*, *Philos. Mag. B* **81**, 793 (2001).
- [7] A. Ceulemans, and P. W. Fowler, *J. Chem. Phys.* **93**, 1221 (1990).
- [8] N. Manini and P. De Los Rios, *Phys. Rev. B* **62**, 29 (2000).
- [9] C. P. Moate *et al.*, *Phys. Rev. Lett.* **77**, 4362 (1996).
- [10] M. Lüders *et al.*, *Philos. Mag. B* **82**, 1611 (2002).
- [11] P. H. Butler, *Point Group Symmetry Applications* (Plenum, New York, 1981).
- [12] A. A. Stuchebrukhov and R. A. Marcus, *J. Chem. Phys.* **98**, 6044 (1993).
- [13] J. Jaklic and P. Prelovsek, *Adv. Phys.* **49**, 1 (2000).
- [14] J. L. Hubbard and D. L. Lichtenberger, *J. Chem. Phys.* **75**, 2560 (1981).
- [15] L. Martinelli *et al.*, *Phys. Rev. B* **43**, 8395 (1991).
- [16] I. B. Bersuker and V. Z. Polinger, *Vibronic Interactions in Molecules and Crystals* (Springer-Verlag, Berlin, 1989), Sect. 4.1.
- [17] P. Baltzer *et al.*, *Chem. Phys.* **224**, 95 (1997).
- [18] D. R. Miller, *Atomic and Molecular Beam Methods* ed. by G. Scoles, (Oxford University Press, Oxford 1988), Ch. 2.
- [19] O. Gunnarsson *et al.*, *Phys. Rev. Lett.* **74**, 1875 (1995); O. Gunnarsson, *Phys. Rev. B* **51**, 3493 (1995).
- [20] R. D. Bendale *et al.*, *Chem. Phys. Lett.* **194**, 467 (1992).
- [21] M. Saito, *Phys. Rev. B* **65**, 220508 (2002).
- [22] Another DF calculation [21] based on a different functional yielded couplings roughly in the same range. However we could not re-compute the PE spectrum with these couplings due to their lack of distinction between coupling contributions of type $r = 1$ and $r = 2$.
- [23] The tier size increases quickly, but we cut it off by

including up to some given number N_{\max} of states per tier, according to their perturbative weight $w_b = \sum_a f \left(\langle b | \hat{H}_{e-v} | a \rangle [E_a - E_b]^{-1} \right) w_a$ where $f(x) = (1 + x^{-2})^{-\frac{1}{2}}$, the sum extends over all the states $|a\rangle$ in the

previous tier, and the weight of $\hat{c}_{m\sigma}^\dagger |i\rangle$ is taken as unity. [24] This, incidentally, rules out the possibility to observe tunnel split states [4] in PE, as they necessarily possess *different* symmetries.